hep-ph/0304215

A_{FB}^b and R_b at LEP and New Right-Handed Gauge Bosons

Xiao-Gang He*

Department of Physics

National Taiwan University

Taipei, Taiwan 10764, R.O.C.

G. Valencia†

Department of Physics

Iowa State University

Ames, IA 50011

(Dated: June 4, 2005)

Abstract

We explore models with additional right-handed gauge bosons that couple predominantly to the third generation in the context of $b\bar{b}$ production at LEP. In particular we investigate potential new contributions to δg_{Rb} that are needed if the measured A_{FB}^b at the Z peak is interpreted as a signal of new physics. We identify two sources of large δg_{Rb} corrections: $Z - Z'$ mixing at tree-level, and one-loop effects from a new $SU_R(2)$ triplet of gauge bosons. We find that the latter can contribute to δg_{Rb} at the 1%-level. We place bounds on the mass of the additional Z' gauge boson that occurs in these models using the R_b measurements from LEP-II. We find that even in cases where the Z' couples almost exclusively to the b and t-quarks, masses lighter than about 500 GeV are already excluded.

*hexg@phys.ntu.edu.tw

†valencia@iastate.edu

I. INTRODUCTION

The precision measurements at the Z resonance continue to exhibit a deviation from the standard model in the observable A_{FB}^b by about -3.2 standard deviations [1, 2]. At the same time R_b deviates from the standard model by only 1.4 standard deviations [2]. It has been pointed out by Chanowitz [3, 4] that the deviation in A_{FB}^b presents a problem for the standard model whether it is genuine or not. In particular, Chanowitz argues that if the anomaly in A_{FB}^b is attributed to systematic error and dropped from the LEP fits, then the indirect determination of the Higgs mass is in conflict with the direct limit [3, 4]. One possible interpretation of this result is that there is new physics associated with the $Zb\bar{b}$ couplings, and we explore this possibility in the context of non-universal right-handed interactions.

We adopt the following notation for the effective couplings between the Z-boson and the b and t quarks,

$$\mathcal{L} \;=\; -\frac{g}{2\cos\theta_W}\bar{f}\gamma^\mu\left[\left(g_{Lf}+\delta g_{Lf}\right)P_L+\left(g_{Rf}+\delta g_{Rf}\right)P_R\right]f Z_\mu, \tag{1}$$

with $P_{L,R} = (1 \mp \gamma_5)/2$, and tree-level standard model couplings g_{Lf} and g_{Rf} as in the Appendix. In terms of these effective couplings, the results in Ref.[1] suggest that new physics could be responsible for as much as $\delta g_{Rb} \sim 0.04$, $\delta g_{Lb} \sim 0.004$. At the same time, new physics contributions to the τ-lepton couplings are constrained to be at most at the 0.001 level.

Several discussions of new physics effects regarding A_{FB}^b or R_b have appeared in the literature. Among them: light SUSY partners [5]; quark mixing with new fermions [6, 7, 8, 9]; top-color [10, 11, 12]; top-flavor [13, 14, 15, 16]; and non-universal left-right models [17]. Our goal in this paper is to extend our results in Ref. [17] by computing the dominant one-loop effects to δg_{Rb}, and by using the LEP-II data on $e^+e^- \to b\bar{b}$ to constrain the mass of the new gauge bosons.

In the standard model the one-loop corrections to δg_{Lb} that are proportional to M_t^2 are approximately 0.006 [18]. We can use this result as a benchmark for δg_{Rb} from new physics, suggesting that if it is to occur at one-loop there must be an enhancement relative to the standard model electroweak corrections. This is precisely what can occur in models such as those we discussed in Ref. [17], where the coupling strength of the new right-handed

interaction, g_R, is significantly larger than the $SU(2)_L$ coupling g_L. In this paper we calculate these corrections in a simple case and find that δg_{Rb} from one-loop effects can be 1%.

Our paper is organized as follows. In Section II we describe models with additional right-handed gauge bosons that could change the value δg_{Rb} significantly while respecting other phenomenological constraints. In particular we discuss several ways in which the predominant effects occur for the b and t-quark couplings but not for the τ-lepton couplings through $Z - Z'$ mixing. In Section III we show how, even in the absence of $Z - Z'$ mixing, one-loop contributions to δg_{Rb} can occur at the 1%-level. In Section IV we present bounds on the mass of the new gauge bosons from the process $e^+e^- \to b\bar{b}$ at LEP-II. We state our conclusions in Section V and relegate some details to the Appendix.

II. NON-UNIVERSAL LEFT-RIGHT MODELS

The models to be discussed are variations of left-right models [19, 20] in which the right-handed interactions single out the third generation. Our basic model was introduced in Ref. [17] and we start by recalling its salient features. The gauge group of the model is $SU(3)\times SU(2)_L\times SU(2)_R\times U(1)_{B-L}$ with gauge couplings g_3, g_L, g_R and g, respectively. The model differs from other left-right models in the transformation properties of the fermions.

The first two generations are chosen to have the same transformation properties as in the standard model with $U(1)_Y$ replaced by $U(1)_{B-L}$,

$$\begin{aligned} &Q_L = (3,2,1)(1/3), \quad U_R = (3,1,1)(4/3), \quad D_R = (3,1,1)(-2/3), \\ &L_L = (1,2,1)(-1), \quad E_R = (1,1,1)(-2). \end{aligned} \tag{2}$$

The numbers in the first parenthesis are the $SU(3)$, $SU(2)_L$ and $SU(2)_R$ group representations respectively, and the number in the second parenthesis is the $U(1)_{B-L}$ charge.

The third generation is chosen to transform differently,

$$\begin{aligned} &Q_L(3) = (3,2,1)(1/3), \quad Q_R(3) = (3,1,2)(1/3), \\ &L_L(3) = (1,2,1)(-1), \quad L_R = (1,1,2)(-1). \end{aligned} \tag{3}$$

The above assignments are unusual compared with the conventional left-right model, but they enhance the difference between the right handed couplings of the first two and the third generations. This model is anomaly free.

The correct symmetry breaking and mass generation of particles can be induced by the vacuum expectation values of three Higgs representations: $H_R = (1,1,2)(-1)$, whose non-zero vacuum expectation value (vev) v_R breaks the group down to $SU(3)\times SU(2)\times U(1)$; and the two Higgs multiplets, $H_L = (1,2,1)(-1)$ and $\phi = (1,2,2)(0)$, which break the symmetry to $SU(3)\times U(1)_{em}$. For the purpose of symmetry breaking, only one of H_L or ϕ is sufficient, but both are required to give masses to all fermions. It is possible to introduce additional Higgs representations as mentioned in Ref. [17], but we will not do so in this paper.

The introduction of ϕ causes the standard model W_L and Z_o to mix with the new W_R and Z_R gauge bosons. Here W_R is the $SU(2)_R$ charged gauge boson and Z_R is a linear combination of the neutral component of the $SU(2)_R$ gauge boson W_{3R} and the $U(1)_{B-L}$ gauge boson B. Specifically,

$$\begin{aligned} Z_o &= \cos\theta_W W_{3L} - \sin\theta_W \cos\theta_R B - \sin\theta_W \sin\theta_R W_{3R}, \\ Z_R &= \cos\theta_R W_{3R} - \sin\theta_R B, \end{aligned} \tag{4}$$

where $\tan\theta_R = g/g_R$.

In the bases $(W_L,\ W_R)$ and $(Z_o,\ Z_R)$ for the massive gauge bosons, the mass matrices were given in Ref. [17] and we reproduce them here for later convenience:

$$\begin{aligned} m^2_{11W} &= \frac{1}{2}g_L^2(|v_L|^2+|v_1|^2+|v_2|^2),\ m^2_{22W} = \frac{1}{2}g_R^2(|v_R|^2+|v_1|^2+|v_2|^2), \\ m^2_{12W} &= -g_L g_R Re(v_1 v_2^*),\ m^2_{11Z} = \frac{1}{2}\frac{g_L^2}{\cos^2\theta_W}(|v_L|^2+|v_1|^2+|v_2|^2), \\ m^2_{22Z} &= \frac{1}{2}\frac{g_R^2}{\cos^2\theta_R}(|v_L|^2\sin^4\theta_R + (|v_1|^2+|v_2|^2)\cos^4\theta_R + |v_R|^2), \\ m^2_{12Z} &= \frac{1}{4}g_L g_R \frac{\sin\theta_R}{\cos\theta_W}(|v_L|^2\tan\theta_R - (|v_1|^2+|v_2|^2)\cot\theta_R)). \end{aligned} \tag{5}$$

After diagonalization of the mass-squared matrices, the lighter and heavier mass eigenstates $(Z,\ Z')$ and $(W,\ W')$ are given by

$$\begin{pmatrix} W \\ W' \end{pmatrix} = \begin{pmatrix} \cos\xi_W & \sin\xi_W \\ -\sin\xi_W & \cos\xi_W \end{pmatrix}\begin{pmatrix} W_L \\ W_R \end{pmatrix}, \quad \begin{pmatrix} Z \\ Z' \end{pmatrix} = \begin{pmatrix} \cos\xi_Z & \sin\xi_Z \\ -\sin\xi_Z & \cos\xi_Z \end{pmatrix}\begin{pmatrix} Z_o \\ Z_R \end{pmatrix}, \tag{6}$$

where $\xi_{Z,W}$ are the mixing angles,

$$\tan(2\xi_{W,Z}) = \frac{2m^2_{12(W,Z)}}{m^2_{11(Z,W)} - m^2_{22(Z,W)}}. \tag{7}$$

In this model there are new interactions between the massive gauge bosons and quarks. For the charged current interaction, there are both left and right handed interactions. In the weak eigenstate basis, the charged gauge boson, W_L, couples to all generations, but the charged gauge boson, W_R, only couples to the third generation. There is a similar pattern for the neutral gauge interactions. This pattern gives rise to interactions between the fermions and the lightest physical gauge bosons that can be made to resemble the standard model couplings plus enhanced right-handed couplings for the third generation. In the mass eigenstate basis the quark-gauge-boson interactions are given by,

$$\begin{aligned}\mathcal{L}_W &= -\frac{g_L}{\sqrt{2}}\bar{U}_L\gamma^\mu V_{KM} D_L(\cos\xi_W W_\mu^+ - \sin\xi_W W_\mu^{'+}) \\ &\quad -\frac{g_R}{\sqrt{2}}\bar{u}_{Ri}\gamma^\mu V^{u*}_{Rti}V^d_{Rbj}d_{Rj}(\sin\xi_W W_\mu^+ + \cos\xi_W W_\mu^{'+}) \;+\; \text{h. c.},\end{aligned} \tag{8}$$

where $U = (u,\ \ c,\ \ t)$ and $D = (d,\ \ s,\ \ b)$. V_{KM} is the Kobayashi-Maskawa mixing matrix and $V^{u,d}_{Rij}$ are unitary matrices which rotate the right handed quarks u_{Ri} and d_{Ri} from the weak eigenstate basis to the mass eigenstate basis. The repeated indices i and j are summed over three generations. For the neutral sector the couplings are,

$$\begin{aligned}\mathcal{L}_Z &= -\frac{g_L}{2\cos\theta_W}\bar{q}\gamma^\mu(g_V - g_A\gamma_5)q(\cos\xi_Z Z_\mu - \sin\xi_Z Z'_\mu) \\ &+ \frac{g_Y}{2}\tan\theta_R(\frac{1}{3}\bar{q}_L\gamma^\mu q_L + \frac{4}{3}\bar{u}_{Ri}\gamma^\mu u_{Ri} - \frac{2}{3}\bar{d}_{Ri}\gamma^\mu d_{Ri})(\sin\xi_Z Z_\mu + \cos\xi_Z Z'_\mu) \\ &- \frac{g_Y}{2}(\tan\theta_R + \cot\theta_R)(\bar{u}_{Ri}\gamma^\mu V^{u*}_{Rti}V^u_{Rtj}u_{Rj} - \bar{d}_{Ri}\gamma^\mu V^{d*}_{Rbi}V^d_{Rbj}d_{Rj})(\sin\xi_Z Z_\mu + \cos\xi_Z Z'_\mu)\end{aligned} \tag{9}$$

In this expression, $g_Y = g\cos\theta_R = g_R\sin\theta_R$, q and q_L are summed over u, d, c, s, t, b quarks, and repeated i, j indices are summed over the three generations. The first line contains the standard model couplings to the Z in the limit $\xi_Z = 0$. The first two lines also contain couplings of the two Z bosons to quarks that arise through mixing of the neutral gauge bosons.

Similarly, the couplings to leptons are given, in the weak eigenstate basis, by:

$$\begin{aligned}\mathcal{L}_Z(lepton) &= -\frac{g_L}{2\cos\theta_W}\bar{\ell}\gamma^\mu(g_V - g_A\gamma_5)\ell(\cos\xi_Z Z_\mu - \sin\xi_Z Z'_\mu) \\ &+ \frac{g_Y}{2}\tan\theta_R(-\bar{\ell}_L\gamma^\mu\ell_L - 2\bar{E}_{Ri}\gamma^\mu E_{Ri})(\sin\xi_Z Z_\mu + \cos\xi_Z Z'_\mu) \\ &- \frac{g_Y}{2}(\tan\theta_R + \cot\theta_R)(\bar{\nu}_{R\tau}\gamma^\mu\nu_{R\tau} - \bar{\tau}_R\gamma^\mu\tau_R)(\sin\xi_Z Z_\mu + \cos\xi_Z Z'_\mu).\end{aligned} \tag{10}$$

In this case, ℓ and ℓ_L are summed over $e,\ \mu,\ \tau,\ \nu_e,\ \nu_\mu,\ \nu_\tau$ and E_R are summed over three generations.

The most interesting terms in Eqs. 9 and 10 occur in the third line and are potentially large if $\cot\theta_R$ is large. In the weak interaction basis they affect only the third generation whereas in the mass eigenstate basis (as written in Eq. 9) they also give rise to flavor changing neutral currents. To satisfy the severe constraints that exist on flavor changing neutral currents we have to require that the V_R^d and V_R^u matrices be nearly diagonal.

In Ref. [17] we studied the case with $\xi_Z \neq 0$, in which $Z - Z'$ mixing is responsible for the shifts in the effective right-handed coupling of the b-quark. Within this scenario, the model given above also induces large shifts in the right-handed coupling of the τ-lepton, making it phenomenologically unacceptable. One finds for large $\cot\theta_R$[23],

$$\begin{aligned}
\delta g_{Rb} &\approx -\sin\theta_W \cot\theta_R V_{Rbb}^{d*} V_{Rbb}^{d}\, \xi_Z \\
\delta g_{Rt} &\approx \sin\theta_W \cot\theta_R V_{Rtt}^{u*} V_{Rtt}^{u}\, \xi_Z \\
\delta g_{R\tau} &\approx -\sin\theta_W \cot\theta_R\, \xi_Z .
\end{aligned} \tag{11}$$

This last equation constrains the product $\cot\theta_R\xi_Z$ to be at the 10^{-3} level or less, whereas one would need $\cot\theta_R\xi_Z \sim 0.08$ [17] to explain A_{FB}^b through this mechanism. Nevertheless, there are several ways around this constraint. One possibility is to eliminate the relation between the b-quark and τ-lepton couplings to the new gauge bosons. To maintain a model that is anomaly free, this is accomplished by introducing additional fermions and can be done in more than one way. Two examples are given below. A second possibility is to require the $Z - Z'$ mixing to be small (or zero) and in this way satisfy the constraints from τ leptons. As we discuss in Section III, there is a second mechanism at the loop level by which the model can induce significant shifts on δg_{Rb} and not on $\delta g_{R\tau}$.

We now discuss two ways to modify the model so that it remains anomaly free but does not have enhanced couplings for the τ-lepton in the case of large $\cot\theta_R$

A. Modified lepton sector

In this first example we keep the quark sector as above but make some modifications to the lepton content. The lepton sector consists of the usual three generations (all transforming as in Eq. 2) plus

$$L_R = \begin{pmatrix} \nu'_R \\ e'_R \end{pmatrix} = (1,1,2)(-1), e'_L = (1,1,1)(-2). \tag{12}$$

Compared with the particle content of Eq. 2 and 3, the net new particles are e'_L and $E_R(3)$. Their contributions to gauge anomaly cancel each other, and therefore the theory is anomaly free.

The new particle e' can be made heavy because H_R provides its mass. The neutral new particle ν'_R can be made heavy by introducing a $\Delta_R(1,1,3)(-2)$ Higgs representation with large VEV. Therefore, at low energy one does not need to consider the effect of the new fermions.

The couplings for the usual three generations of leptons become,

$$\begin{aligned}\mathcal{L}_Z(lepton) &= -\frac{g_L}{2\cos\theta_W}\bar{\ell}\gamma^\mu(g_V - g_A\gamma_5)\ell(\cos\xi_Z Z_\mu - \sin\xi_Z Z'_\mu) \\ &+ \frac{g_Y}{2}\tan\theta_R(-\bar{\ell}_L\gamma^\mu\ell_L - 2\bar{E}_{Ri}\gamma^\mu E_{Ri})(\sin\xi_Z Z_\mu + \cos\xi_Z Z'_\mu). \qquad (13)\end{aligned}$$

Once again ℓ and ℓ_L are summed over $e,\ \mu,\ \tau,\ \nu_e,\ \nu_\mu,\ \nu_\tau$ and E_R is summed over three generations. The couplings of the new leptons are

$$\begin{aligned}\mathcal{L}_Z(lepton) &= -\frac{g_R}{\sqrt{2}}[\bar{\nu}'_R\gamma_\mu e'_R W_R^\mu + H.c.] \\ &- \frac{g_L}{2\cos\theta_W}(-2q\sin^2\theta_W)\bar{e}'\gamma^\mu e'(\cos\xi_Z Z_\mu - \sin\xi_Z Z'_\mu) \\ &+ \frac{g_Y}{2}\tan\theta_R(-2\bar{e}'\gamma^\mu e')(\sin\xi_Z Z_\mu + \cos\xi_Z Z'_\mu) \\ &- \frac{g_Y}{2}(\tan\theta_R + \cot\theta_R)(\bar{\nu}'_R\gamma^\mu\nu'_R - \bar{e}'_R\gamma^\mu e'_R)(\sin\xi_Z Z_\mu + \cos\xi_Z Z'_\mu). \qquad (14)\end{aligned}$$

B. Modified quark sector

In this case we have three generations of leptons transforming as in Eq. 2 with couplings as in Eq. 13, and we introduce additional quarks to cancel the anomalies:

$$Q'_L = \begin{pmatrix} u'_L \\ d'_L \end{pmatrix} = (3,1,2)(1/3), u'_R = (3,1,1)(4/3), d'_R = (3,1,1)(-2/3). \qquad (15)$$

The usual three generations of quarks have the same quantum numbers as in Eqs. 2, 3 and couplings as in Eqs. 8, 9. Again the above particle content gives a gauge anomaly free theory, and the new particles can be made heavy because they receive their mass from the VEV of H_R. The new quarks have couplings,

$$\mathcal{L}_Z(quark) = -\frac{g_L}{2\cos\theta_W}(-2q\sin^2\theta_W)\bar{q}'\gamma^\mu q'(\cos\xi_Z Z_\mu - \sin\xi_Z Z'_\mu)$$

$$+ \frac{g_Y}{2}\tan\theta_R(\frac{4}{3}\bar{u}'\gamma^\mu u' - \frac{2}{3}\bar{d}'\gamma^\mu d')(\sin\xi_Z Z_\mu + \cos\xi_Z Z'_\mu)$$
$$- \frac{g_Y}{2}(\tan\theta_R + \cot\theta_R)(\bar{u}'_L\gamma^\mu u'_L - \bar{d}'_L\gamma^\mu d'_L)(\sin\xi_Z Z_\mu + \cos\xi_Z Z'_\mu). \quad (16)$$

C. Discussion

The previous two examples illustrate how it is possible to single out the b and t-quarks with a new right-handed interaction without affecting the τ lepton very much. The price paid is, of course, the introduction of additional fermions. The additional fermions can be made heavy and this allows us to ignore them at this stage, where we are interested only in the effect of potentially strong right-handed couplings of the b and t quarks in LEP observables. The new heavy fermions are only used to illustrate that it is possible to construct a renormalizable, anomaly free, model of this type.

The couplings of the b-quark to the new right-handed gauge bosons remain as in the original model so that, according to Eq.11, we require $\xi_Z \cot\theta_R \sim 0.08$ to explain A^b_{FB} [17] through $Z - Z'$ mixing. With $\cot\theta_R$ large, the new physics effects mainly affect the third generation of quarks; our model is in some sense "leptophobic".

In Ref. [17], we pointed out that the process $b \to s\gamma$ severely constrains the mixing of the charged gauge bosons ξ_W. This constraint is not in conflict with the mixing needed in the neutral sector, ξ_Z, to fit A^b_{FB} as discussed in Ref. [17]. Here we point out that there is another way to obtain Eq. 11 without affecting $b \to s\gamma$. This involves a new model in which the $SU(2)_R$ is replaced by a $U(1)_R$ with up quarks (leptons) and down quarks (leptons) in $SU(2)_R$ doublets carrying 1 and -1 of $U(1)_R$ charges, respectively. This model will also give $\delta g_{Rb} \sim \xi_Z \cot\theta_R$ as in Eq. 11, but it now arises in the context of models where (a) there are no large contributions to $Z \to \tau^+\tau^-$, and (b) there are no new charged gauge bosons W', so that there are no constraints from $b \to s\gamma$. The contributions to the parameter T that occur through mixing of the Z and Z' are identical to Ref. [17] and lead to the allowed region of Figure 1 in that reference.

The most important new feature common to all the models that we have discussed is the existence of a new Z' gauge boson which has enhanced couplings to top and bottom quarks (and perhaps to the τ-lepton provided its mixing with the Z is sufficiently small). In Section IV we explore the bounds that exist on the mass of this Z' from LEP-II measurements.

III. ONE-LOOP CONTRIBUTIONS TO δg_{Rb}

In models like the ones presented in Section II, with a new $SU(2)_R$ gauge interaction, there is a one-loop contribution to δg_{Rb} that is present even when there is no mixing. A priori we can expect this contribution to be similar in size to the standard model contribution to δg_{Lb} proportional to M_t^2. One can imagine a suppression of the form $(M_W/M_{W_R})^2$ with respect to the standard model δg_{Lb}, but this can be compensated by an enhancement $(g_R/g_L)^2 \sim \cot^2\theta_R$ in the right-handed gauge couplings.

It would be impossible to present a complete one-loop calculation for $Z \to b\bar{b}$ in the general case of Section II because we do not have sufficient information at present to determine all the parameters in those models. At the same time, we are interested in exploring the idea of a potentially strong right-handed interaction affecting the b and t-quarks more than we are interested in the specific details of the models in Section II. For this reason, we consider a slightly simpler calculation that has the ingredients we need. First, we will only concern ourselves with the one-loop corrections that are enhanced by $(g_R/g_L)^2$ with respect to one-loop electroweak corrections. Second, we will require that there be no $Z - Z'$ nor $W - W'$ mixing in the model. Finally, we will treat all standard model fermions as massless except for the top-quark.

A. Model with no tree-level mixing

To eliminate the tree-level mixing in the models of Section II in a simple manner we first require $v_2 = 0$ in Eq. 5. This immediately makes $\xi_W = 0$ and allows us to simplify the notation by calling the remaining VEV in ϕ $v \equiv v_1$. We further make $\xi_Z = 0$ at tree-level by imposing the condition,

$$v_L = v \cot\theta_R \tag{17}$$

in Eq. 5. The parameter ξ_Z describing the $Z - Z'$ mixing is the only one (beyond those already appearing in the standard model) that enters the result for the $Z \to b\bar{b}$ partial width at tree-level. As such, it is the only new parameter that needs to be defined at one-loop in our calculation of $Z \to b\bar{b}$, and we will return to this point at the end of the section.

In the simplified model, the gauge boson masses become,

$$M_W^2 = \frac{g_L^2}{2}\left(v_L^2 + v^2\right) = \frac{g_R^2}{2\tan^2\theta_W}v^2 \ , \ M_Z^2 = \frac{M_W^2}{\cos^2\theta_W}$$

$$M_{W_R}^2 = \frac{g_R^2}{2}\left(v_R^2 + v^2\right) \ , \ M_{Z_R}^2 = \frac{g_R^2}{2}\left(\frac{v_R^2}{\cos^2\theta_R} + v^2\right) \tag{18}$$

so that $M_{W_R} \approx M_{Z_R}$ for large $\cot\theta_R$ (and equal to $M_{W'}$ and $M_{Z_\prime}$ since in this case there is no mixing). Recalling the relation, $g_R \sin\theta_R = g_L \tan\theta_W$, we see that this sector of the model is characterized by the two ratios of vevs

$$\frac{v_L}{v} = \cot\theta_R \ , \ \frac{v_R}{v} \approx \frac{M_{W_R}}{M_W \tan\theta_W} \tag{19}$$

where the last expression follows for $v_R/v >> 1$. It will also be convenient to define $x_v = v^2/(v^2 + v_R^2)$.

In the approximation $m_b = 0$, the Yukawa Lagrangian necessary to generate the top-quark mass is given by,

$$\mathcal{L}_Y = -\kappa \begin{pmatrix} \bar{t}_L & \bar{b}_L \end{pmatrix} \phi \begin{pmatrix} t_R \\ b_R \end{pmatrix} + \text{h.c.} \tag{20}$$

All the couplings in this Yukawa potential can thus be written in terms of m_t and v as in Eq. A4.

B. Loops with right-handed gauge bosons

We are ready to calculate the one-loop corrections to δg_{Rb} that are enhanced by $\cot^2\theta_R$. We start by considering the diagrams in Figure 1 that do not involve scalar mesons in the loop. We work in unitary gauge with the vertices given in the Appendix, and we use dimensional regularization with the notation,

$$\frac{1}{\epsilon} = \frac{2}{4-n} - \gamma + \log(4\pi) - \log\ \mu^2 \, . \tag{21}$$

Relegating details for each diagram to the Appendix, we can write a simple analytical result for the sum of the diagrams in Figure 1 in the limit $M_Z = 0$,

$$(\delta g_{Rb})_{GB} = \frac{g_R^2}{16\pi^2}\frac{M_t^2}{M_{W_R}^2}\frac{1}{4}\left(\frac{1}{\epsilon} - \frac{7}{2} - \log\left(\frac{M_t^2}{\mu^2}\right) - 3\log\left(\frac{M_t^2}{M_{W_R}^2}\right)\right) \tag{22}$$

Later on we will show numerical results for $M_Z \neq 0$. Unlike the counterpart of this calculation in the standard model, Eq. 28, Eq. 22 is divergent. This indicates the presence of additional contributions to this process in our model.

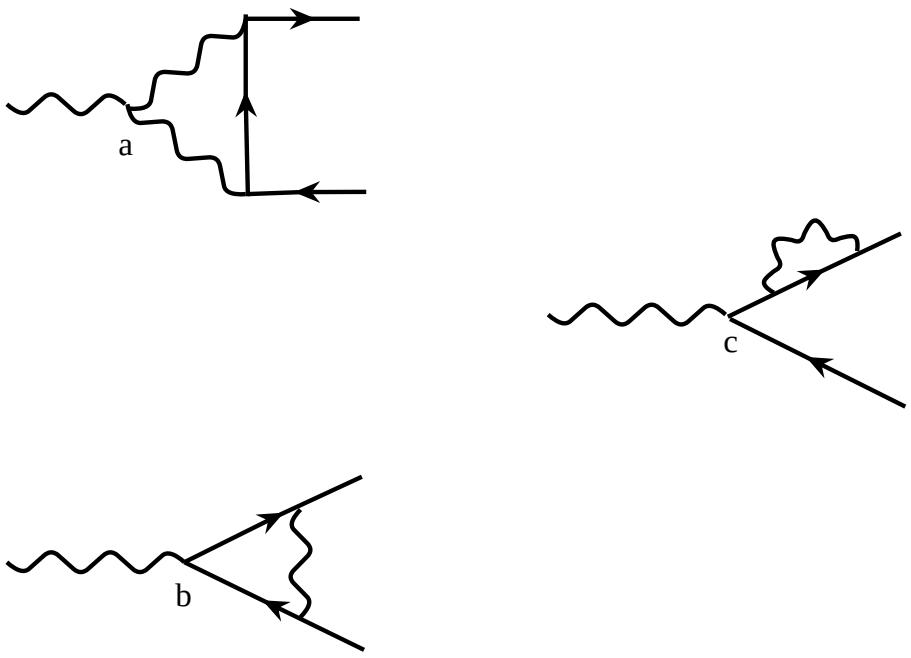

FIG. 1: Unitary gauge Diagrams for $Z \to b\bar{b}$ that do not involve scalars.

There are two additional diagrams of the form of Figure 1 that give corrections to the right-handed coupling and that are enhanced by g_R^2. They look like the diagrams (b) and (c) with an exchange of a Z_R (and therefore b-quarks in the intermediate lines). Both of these turn out to be finite and their finite parts precisely cancel each other out in the $M_Z = 0$ limit.

C. Loops with Scalars

We consider next the contributions from diagrams in which scalars appear in the loops, as in Figure 2.

The finite part that results from these diagrams is model dependent. In particular it depends on the details of the scalar potential, which we have not specified, and which determines the masses of the physical scalar and pseudo-scalar mesons present in the model. We are only interested here in estimating the size of the vertex corrections in Figure 1, and wish to consider the diagrams in Figure 2 only insofar as they are needed to render the result finite. For this purpose it is sufficient to identify a basis for the scalars that is orthogonal to the would-be-Goldstone bosons that give the gauge bosons their mass. We consider all

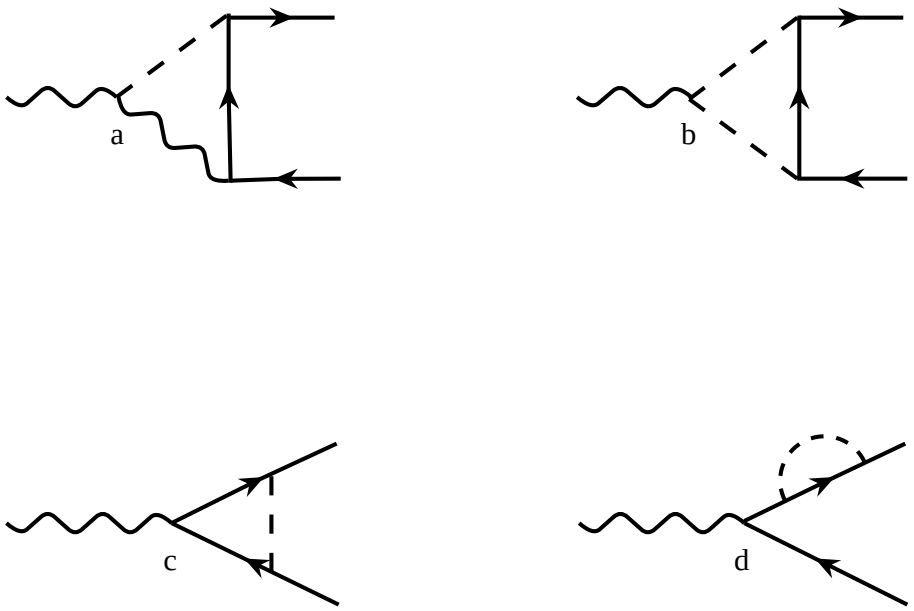

FIG. 2: $Z \to b\bar{b}$ one-loop diagrams involving scalars

physical scalars to be degenerate and to have a large mass, of order M_{W_R}. With details relegated to the Appendix, we find that the sum of these diagrams contributes the following terms that are enhanced by $\cot^2\theta_R$,

$$\begin{aligned}(\delta g_{Rb})_S &= \frac{1}{16\pi^2}\left(\frac{m_t}{v}\right)^2\left(-\frac{1}{2}x_v(1-x_v)\right)\left(\frac{1}{\epsilon}-\log\left(\frac{M_H^2}{\mu^2}\right)+\frac{5}{2}\right)\\ &= \frac{g_R^2}{16\pi^2}\frac{M_t^2}{M_{W_R}^2}\frac{1}{4}\left(-\frac{1}{\epsilon}+\log\left(\frac{M_H^2}{\mu^2}\right)-\frac{5}{2}\right)\end{aligned} \tag{23}$$

Notice that the left-handed coupling δg_{Lb} does not receive corrections from the sum of diagrams in Figure 2. With this result, Eq. 23, we find that the divergent terms precisely cancel the left-over ones from the gauge boson sector in Eq. 22 leaving us with a finite answer.

D. Renormalization and $Z - Z'$ Mixing

Finally we comment on the renormalization scheme used. At tree level, the $Z \to b\bar{b}$ decay width (or A_{FB}^b) takes the same value as in the standard model in the absence of $Z - Z'$ mixing. We can therefore express it in terms of the input parameters G_F, the physical Z mass and $\alpha(M_Z)$ as is usually done for the standard model case. It is clear from the vertices given in the Appendix, Section A 3, that none of these quantities receives one-loop corrections

that are enhanced by $\cot^2\theta_R$. The only input parameter that receives enhanced corrections is the $Z - Z'$ mixing angle ξ_Z through diagrams such as those in Figure 3. These diagrams (and a few others), have an enhancement of $\cot\theta_R$ through the $Z't\bar{t}$ or $Z'b\bar{b}$ coupling in the first case and through the $W_R^+ W_R^- Z'$ coupling in the second case. When the Z' line is connected to $b\bar{b}$, a second $\cot\theta_R$ factor is picked up leading to corrections in $Z \to b\bar{b}$ that are enhanced by $\cot^2\theta_R$. In view of this, our simplest option is to adopt a renormalization

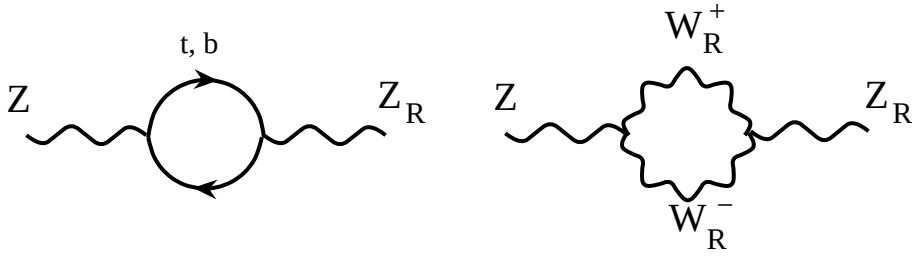

FIG. 3: $Z - Z'$ Mixing at one-loop

scheme in which $\xi_Z \equiv 0$ at one-loop. That is, we absorb the corrections from Figure 3 into the definition of ξ_Z. This completes the discussion of all the one-loop corrections needed to yield a finite δg_{Rb} and we now turn our attention to its possible size.

E. Numerical Results

Adding the results from all diagrams discussed above, we find in the $M_Z = 0$ limit,

$$\delta g_{Rb} = \frac{g_R^2}{16\pi^2}\frac{M_t^2}{M_{W_R}^2}\frac{1}{4}\left(-6 + 3\log\left(\frac{M_{W_R}^2}{M_t^2}\right) + \log\left(\frac{M_H^2}{M_t^2}\right)\right). \tag{24}$$

To illustrate the magnitude of this correction consider the case,

$$\cot\theta_R = \frac{v_L}{v} \approx \frac{v_R}{v} \sim 10 \tag{25}$$

which implies

$$\frac{g_R^2}{M_{W_R}^2} \approx \frac{g_L^2}{M_W^2} \tag{26}$$

and therefore

$$\delta g_{Rb} = \frac{\sqrt{2}G_F M_t^2}{8\pi^2}\left(-3 + \frac{3}{2}\log\left(\frac{M_{W_R}^2}{M_t^2}\right) + \frac{1}{2}\log\left(\frac{M_H^2}{M_t^2}\right)\right). \tag{27}$$

This is to be compared with the corresponding correction to δg_{Lb} in the standard model which is given by [18]

$$\delta g_{Lb} = \frac{\sqrt{2} G_F M_t^2}{8\pi^2}. \tag{28}$$

This shows that with large $\cot\theta_R$ as in Eq. 25, δg_{Rb} in our model is of the same order as the one-loop correction to δg_{Lb} proportional to M_t^2 in the standard model.

In order to include kinematic effects from $M_Z \neq 0$, we compute the integrals over Feynman parameters numerically. It is convenient to present the result in the form

$$\delta g_{Rb} = \frac{\sqrt{2} G_F M_t^2}{8\pi^2} F_1(M_{W_R}) \tag{29}$$

for the case $g_L^2/M_W^2 \approx g_R^2/M_{W_R}^2$. We show F_1 in Figure 4 a. In the more general case it is convenient to write

$$\delta g_{Rb} = \frac{g_R^2}{32\pi^2} F_2(M_{W_R}) \tag{30}$$

and we show F_2 in Figure 4 b. These results indicate that a contribution to δg_{Rb} at the %

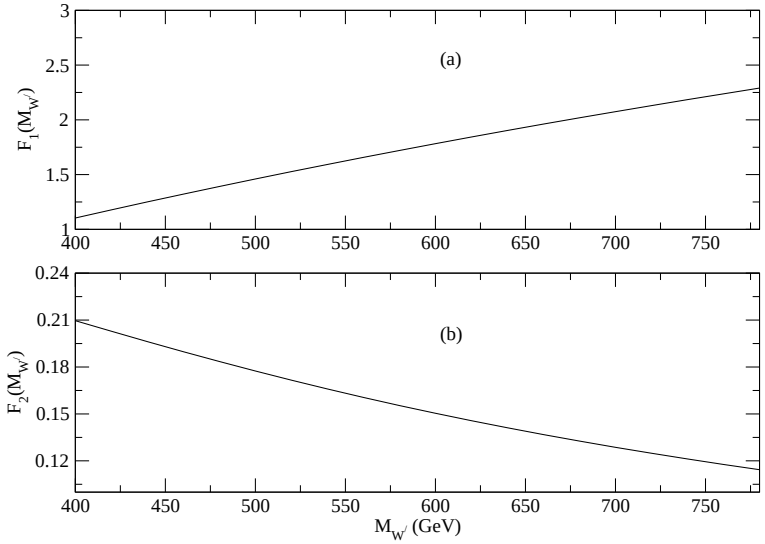

FIG. 4: Form factors $F_1(M_{W_R})$ and $F_2(M_{W_R})$ evaluated numerically to include kinematic effects from a non-zero M_Z for fixed $M_H = 700$ GeV.

level is possible in models with $\cot\theta_R \sim 10$.

IV. CONSTRAINTS FROM LEP-II

The mass of additional Z' gauge bosons that occur in many models is constrained to be larger than about 500 GeV [2]. These bounds arise mostly from processes involving four first or second generation fermions and do not apply to non-universal Z' gauge bosons that couple strongly to third generation fermions but very weakly to first and second generation fermions. Roughly speaking, when a Z' like this is exchanged in a process such as $b\bar{b} \to b\bar{b}$ it generates an amplitude of order electroweak strength times $\cot^2\theta_R$. For the models that we have in mind $\cot\theta_R \sim 10$ this can be a very significant enhancement. On the other hand when the same Z' is exchanged between fermions of the first two generations, in processes such as $u\bar{u} \to u\bar{u}$, it generates an amplitude of electroweak strength times $\tan^2\theta_R$ which is drastically suppressed.

The best bounds one can have at present on such a Z' come from a process in which a first or second generation fermion pair produces a $b\bar{b}$ pair. Since $b\bar{b}$ production in hadron colliders is mostly a strong interaction process, the most promising reaction to constrain our Z' is $e^+e^- \to b\bar{b}$ studied at LEP-II. Notice that for a process such as this one, the exchange of a Z' results in a correction of electroweak strength, suppressed only by the mass of the Z'. The cross-section for this process is largely independent of the value of $\cot\theta_R$. At leading order, $\cot\theta_R$ only appears through the width of the Z' that one must include in the propagator for s-channel exchange.

In this Section we use the LEP-II data on $e^+e^- \to b\bar{b}$ and $e^+e^- \to \tau^+\tau^-$ to constrain the mass of these non-universal Z' gauge bosons. The calculation is performed numerically using the program COMPHEP [21] with the following strategy. We use COMPHEP to calculate tree level cross-sections for $e^+e^- \to f\bar{f}$ at LEP-II energy both for the standard model and for the standard model plus the Z' of Section II. We then use these cross-sections to construct the ratios $R_b/(R_b)_{SM-tree}$ and similarly for A_{FB}^b. We then compare these ratios to the corresponding ratios $(R_b)_{EXP}/(R_b)_{SM}$ where $(R_b)_{EXP}$ are the averages of LEP-II measurements as reported in Ref. [1] and $(R_b)_{SM}$ is the full standard model expectation computed with ZFITTER as reported in Table 8.7 of Ref. [1]. Schematically for the cross-section,

$$\frac{\sigma_{Theory}}{\sigma_{SM}} = \frac{\sigma_{SM-tree} + \sigma_{SM-loop} + \sigma_{Z'}}{\sigma_{SM-tree} + \sigma_{SM-loop}}$$

$$\approx \frac{\sigma_{SM-tree} + \sigma_{Z'}}{\sigma_{SM-tree}} = 1 + \frac{\sigma_{Z'}}{\sigma_{SM-tree}}. \tag{31}$$

In this way the error that results from our using only the tree-level result for the standard model prediction from COMPHEP becomes higher order in our comparison with data.

In models with $Z - Z'$ mixing, we need to remove the enhanced coupling $Z'\tau^+\tau^-$ as discussed in the previous section. In that case the only relevant LEP-II process to bound the Z' is $e^+e^- \to b\bar{b}$. There are two observables that can be used: R_b and A^b_{FB}. In Figure 5 we show $R_b/(R_b)_{SM}$ for different values of M'_Z. In this figure we have assumed no mixing ($\xi_Z = 0$) and used $\cot\theta_R = 15$ [24]. The LEP-II data points are shown with their 1-σ and 3-σ error bars. It is evident already from this figure that $M_{Z'}$ will be constrained to be larger than about 500 GeV.

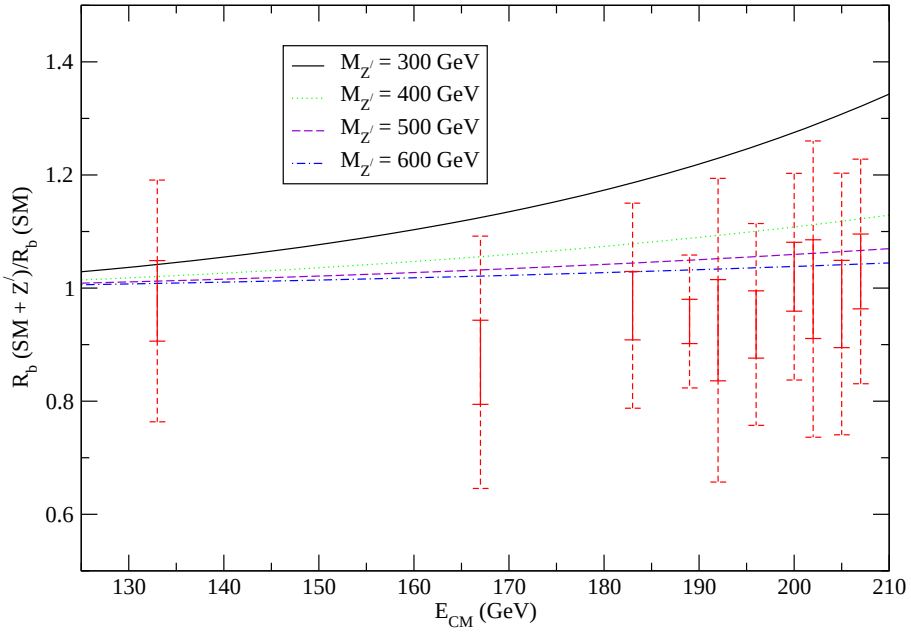

FIG. 5: R_b at LEP-II energies for $\cot\theta_R = 15$ with no $Z - Z'$ mixing. The different curves correspond to $M_{Z'}$ of 300, 400, 500 and 600 GeV. The data points from Ref. [1] are shown with their 1-σ and 3-σ error bars.

In Figure 6 we show similar results for the forward-backward asymmetry. It is evident from this figure that A^b_{FB} does not constrain the Z' as much as R_b does due to its larger experimental error (in this case we only show the 1-σ error-bars).

As discussed in Section II, it is possible to allow $Z - Z'$ mixing in models where the couplings to $\tau^\pm$ are not enhanced. We illustrate the effect of including this mixing in Figure 7.

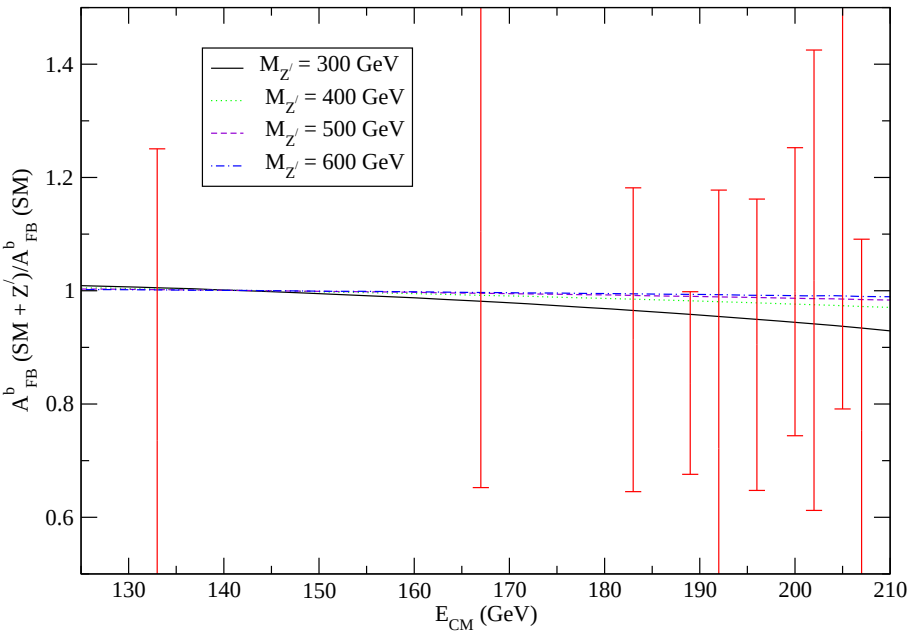

FIG. 6: Same as Figure 5 for A_{FB}^b. Only the 1-σ error bars are shown for the data points from Ref. [1].

For each value of $M_{Z'}$, we have allowed ξ_Z to vary between zero and $\xi_Z = \pm 0.08/\cot\theta_R$, the value required to fit A_{FB}^b from LEP-I. We see that mixing is a small effect on R_b at LEP-II energies.

In Figure 8 we illustrate the effect of varying $\cot\theta_R$ and thus the Z' width for $M_{Z'} = 400$ GeV. We use values $\cot\theta_R = 10$, 15 and also show the result of approximating the Z' exchange with a contact interaction. The results illustrate that below the resonance, the bound on the Z' mass becomes slightly tighter for narrower resonances (smaller $\cot\theta_R$). In our model, the interference between Z and Z' exchange amplitudes is always constructive in the energy region between the two resonances. The figure also illustrates that for a Z' as light as 400 GeV, a contact interaction is a reasonable approximation for effects at LEP-II energies. We shall use this later when comparing our bounds with those extracted by the LEP-II analysis group for contact interactions.

To quantify the bounds on the Z' mass we construct a χ^2 for a fit to LEP-II data with our model. In Figure 9 we present this result after subtracting the χ^2 from a standard model fit (using the ZFITTER results quoted in Ref. [1]). Once again we show the three cases $\cot\theta_R = 10, 15$ and a contact interaction approximation. It is important to notice, for example in

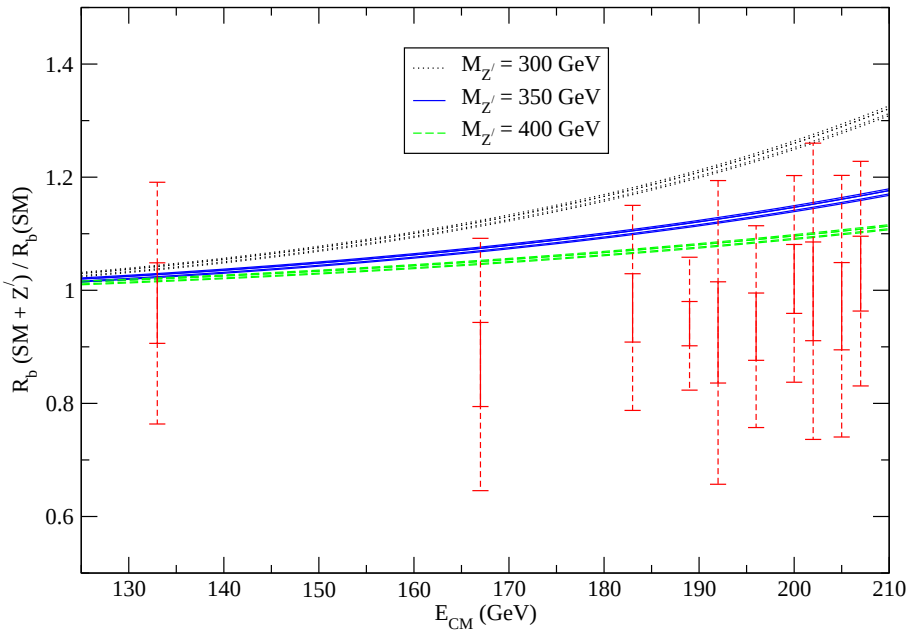

FIG. 7: Same as Figure 5 but allowing for $Z - Z'$ mixing. The bands shown correspond to $\cot\theta_R \xi_z$ ranging from 0 to ± 0.08 with $\cot\theta_R = 15$. For each mass, the upper end of the band corresponds to $\xi_Z = -0.005$ and the lower end of the band corresponds to $\xi_Z = 0.005$. Once again the data points are from Ref. [1].

Figure 5, that the LEP-II data are consistently below the standard model prediction. This, combined with the fact that the interference between the Z and Z' amplitudes in our model is always constructive in this energy region, implies that the standard model is always a better fit than any of our Z' models. If we require that the new model not deviate from the standard model by 2(3) standard deviations, we can place the bounds $M_{Z'} > 700(540)$ GeV for $\cot\theta_R = 15$. Given that the LEP-II data is consistently below the standard model expectation, it is conceivable that there is some common systematic error not accounted for in the quoted error bars. To account for this possibility, we naively rescale the data by a common factor in such a way as to minimize the χ^2 of the standard model fit. Doing this results in lower bounds on the Z' mass. For example, for $\cot\theta_R = 10$ the 2(3) sigma bounds move from 780 (595) GeV to 530 (460) GeV.

We can also use the contact interaction approximation to bound the Z' mass. The

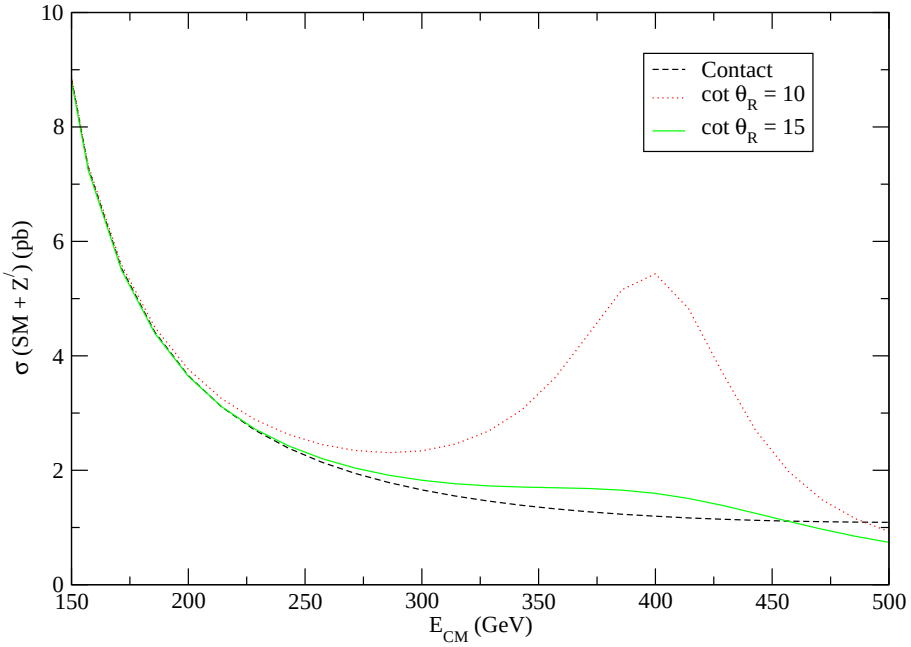

FIG. 8: Cross-section for $e^+e^- \to b\bar{b}$ with $M_{Z'} = 400$ GeV for $\cot\theta_R = 10$, 15 and for a contact interaction approximating the Z' exchange amplitude.

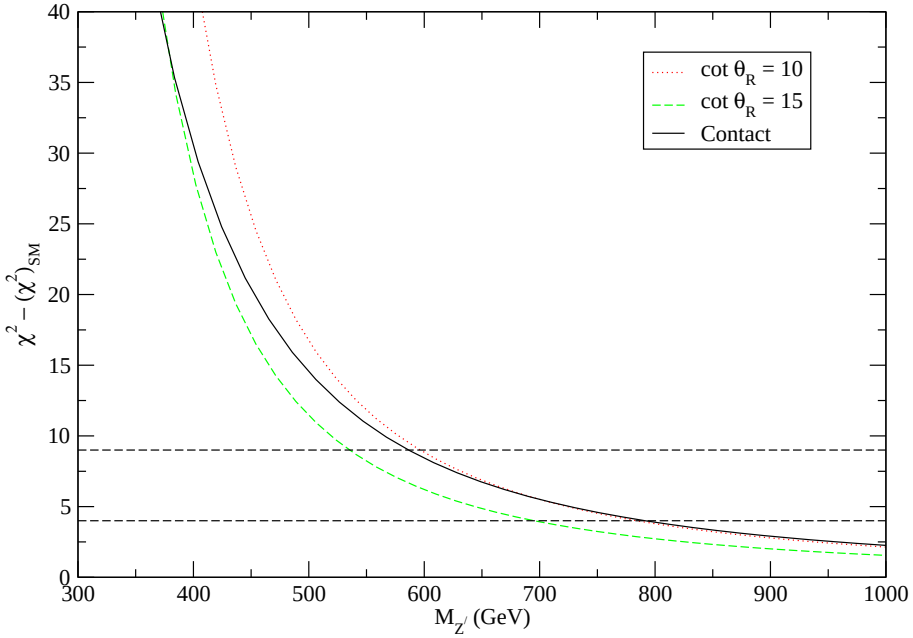

FIG. 9: $\chi^2 - \chi^2_{SM}$ for fits to R_b at LEP-II energies as a function of $M_{Z'}$ setting $\xi_Z = 0$.

correspondence to Table 8.12 of Ref.[1] is (for no mixing),

$$M_{Z'} = \sqrt{\eta}\frac{g_L \tan\theta_W}{4\sqrt{\pi}}\Lambda \tag{32}$$

Our model of Section II generates both a LR contact interaction with $\eta_{LR} = 1$ and a RR contact interaction with $\eta_{RR} = 2$. For constructive interference we thus infer the 95% confidence level bounds $M_{Z'} > 544$ GeV from the RR interaction and $M_{Z'} > 275$ GeV from the LR interaction.

From all this we conclude that in all cases the Z' is already restricted to be heavier than about 500 GeV by LEP-II data.

Finally, since models without mixing also allow large couplings to the τ-lepton, we show in Figure 10 the cross-section for $e^+e^- \to \tau^+\tau^-$ at LEP-II. A calculation of the χ^2 for the fit in this case indicates that the bounds on the Z' mass are slightly higher than those obtained from studying R_b, but not significantly so.

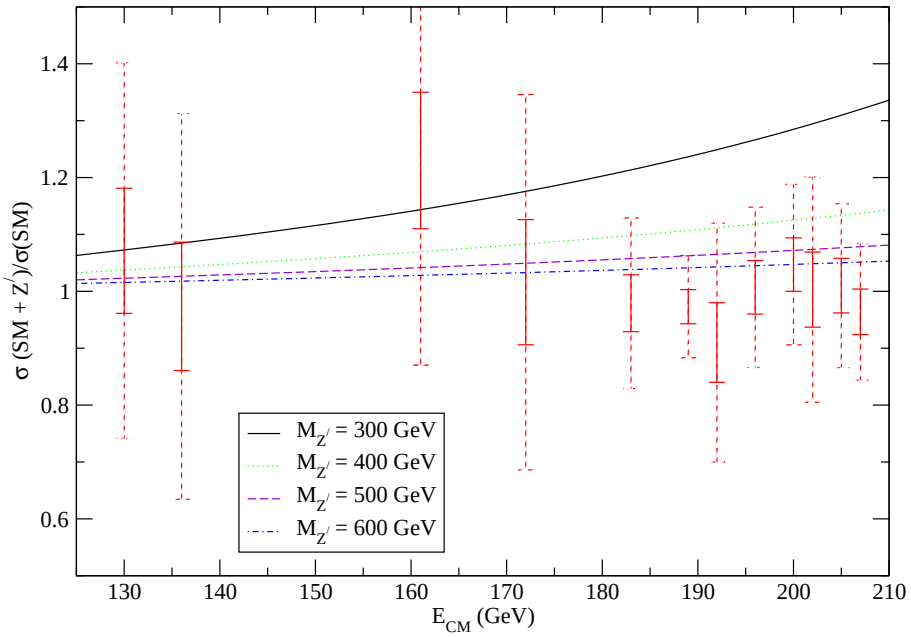

FIG. 10: $\sigma(e^+e^- \to \tau^+\tau^-)$ for $\cot\theta_R = 15$. The data points are from Ref. [1].

V. CONCLUSIONS

Motivated by the 3-σ discrepancy between the standard model prediction and the measured forward-backward asymmetry A_{FB}^b at the Z peak we have studied models which can generate a sufficiently large δg_{Rb} through new non-universal right-handed gauge interactions.

One possible mechanism to generate this δg_{Rb} is the mixing of the Z with a Z'. We had already discussed a model like this in Ref. [17]. In this paper we have illustrated several variations on that model that are also renormalizable and anomaly free. At the cost of introducing additional fermions, we showed two models that produce the required δg_{Rb} while satisfying the LEP constraints on $\delta g_{R\tau}$. We have also indicated how it is possible to modify these models so that they are not constrained by $b \to s\gamma$.

We have identified a second mechanism to generate δg_{Rb} even in cases with no $Z - Z'$ mixing. This occurs in models with an $SU(2)_R$ triplet of gauge bosons at one-loop, and can give rise to δg_{Rb} at the 1% level. By itself, this mechanism is not sufficient to explain the full $\delta g_{Rb} \sim 0.04$ favored by the data. The simple model used to illustrate this effect, provides an example of a renormalizable model that can give rise to relatively large new interactions involving only the b and t quarks while respecting low energy constraints.

Finally we have used the LEP-II data for the process $e^+e^- \to b\bar{b}$ to place bounds on the mass of the Z' in our models. This is a Z' that couples weakly (by a factor $\tan\theta_R \sim 1/10$ weaker than standard electroweak couplings) to fermions of the first two generations. For this reason, standard bounds on Z' gauge bosons do not apply. We find that the LEP-II data constrains it to be heavier than about 500 GeV in all cases.

The contribution of the new gauge bosons in our models to the process $e^+e^- \to b\bar{b}$, is of electroweak strength because the enhancement in the $Z'b\bar{b}$ coupling is compensated by the suppression in the $Z'e^+e^-$ coupling. In this way, our model is an example of a kind of new interactions that will only show their full strength in processes involving four third generation fermions. It may be possible for the LHC to study certain processes of this type, and we are currently investigating this possibility.

Acknowledgments The work of X.G.H. was supported in part by National Science Council under grants NSC 91-2112-M-002-042, and in part by the Ministry of Education Academic Excellence Project 89-N-FA01-1-4-3. The work of G.V. was supported in part by DOE under contract number DE-FG02-01ER41155.

APPENDIX A: VERTICES AND ONE-LOOP RESULTS

1. Basic conventions

The general conventions adopted are:

$$\begin{aligned} g_{Lt} &= 1 - \frac{4}{3}\sin^2\theta_W,\ g_{Rt} = -\frac{4}{3}\sin^2\theta_W, \\ g_{Lb} &= -1 + \frac{2}{3}\sin^2\theta_W,\ g_{Rb} = \frac{2}{3}\sin^2\theta_W, \\ \Gamma_\mu &= -i\frac{g}{2\cos\theta_W}\gamma_\mu\left((g_{Lb}+\delta g_{Lb})P_L + (g_{Rb}+\delta g_{Rb})P_R\right) \\ \frac{1}{\epsilon} &= \frac{2}{4-n} - \gamma + \log(4\pi) - \log\ \mu^2 \end{aligned} \tag{A1}$$

2. Scalar Sector

We start with the following parameterization for the scalars,

$$\begin{aligned} H_L &= \begin{pmatrix} \frac{h_L - i\phi_L}{\sqrt{2}} + v_L \\ \phi_L^- \end{pmatrix},\quad H_R = \begin{pmatrix} \frac{h_R - i\phi_R}{\sqrt{2}} + v_R \\ \phi_R^- \end{pmatrix}, \\ \phi &= \begin{pmatrix} \frac{h_1 - i\phi_1^0}{\sqrt{2}} + v_1 & \phi_1^+ \\ \phi_2^- & \frac{h_2 - i\phi_2^0}{\sqrt{2}} + v_2 \end{pmatrix} \end{aligned} \tag{A2}$$

This parameterization contains both the would-be Goldstone-bosons that give mass to the W, Z, W_R, Z_R and the remaining physical scalar (or pseudo-scalar) particles.

Since we do not specify a scalar potential, we cannot identify the scalar mass eigenstates. Rather we work with a basis of physical scalars chosen to be orthogonal to the would-be Goldstone-bosons, under the simplifying assumption that they all have the same large mass. The physical scalars defined this way are,

$$\begin{aligned} H_1^\pm &= \frac{1}{\sqrt{v^2+v_L^2}}(-v\phi_L^\pm + v_L\phi_2^\pm) \\ H_2^\pm &= \frac{1}{\sqrt{v^2+v_R^2}}(-v\phi_R^\pm + v_R\phi_1^\pm) \\ H_2^0 &= \frac{x}{\sqrt{1+x^2}}(-\sin\theta_R\phi_L^0 + \frac{1}{x}\phi_R^0 + \cos\theta_R\phi_1^0) \\ H_1^0 &= \phi_2^0 \end{aligned} \tag{A3}$$

with $x = v_R/(v\cos\theta_R)$ and with $H_{1,2}^0$ being neutral pseudo-scalars. The only neutral scalar that enters the calculation is the original h_2. Working with this basis we can identify the

divergent contributions arising from diagrams with scalar exchange (they are independent of scalar masses). The finite contributions that depend on the masses of the different scalars can only be obtained after fixing all their masses.

3. Feynman Rules

In unitary gauge, the vertices $\gamma W_L^+ W_L^-$, $\gamma\gamma W_L^+ W_L^-$, $\gamma Z W_L^+ W_L^-$, $Z W_L^+ W_L^-$ and $ZZ W_L^+ W_L^-$ are as in the standard model. The analogous vertices with $W_R^\pm$ taking the place of $W_L^\pm$ can be obtained by multiplying the corresponding vertex with $W_L^\pm$ by a factor of $(-\tan^2\theta_W)$ for each Z. In particular, these vertices are *not* enhanced by g_R/g_L. There are no "mixed" vertices with one W_L and one W_R. For vertices involving a Z_R, the $Z_R W_R^+ W_R^-$ vertex is given by $\tan\theta_W \cot\theta_R/\cos\theta_W$ times the corresponding vertex for $Z W_L^+ W_L^-$ and is, therefore, enhanced with respect to the latter by a factor of $\cot\theta_R$. Finally the $Z Z_R W_R^+ W_R^-$ vertex can be obtained by multiplying the $ZZ W_L^+ W_L^-$ vertex by $-\tan^3\theta_W \cot\theta_R/\cos\theta_W$.

The Feynman rules for couplings of gauge bosons to fermions are already given in Eqs. 8 and 9. The Feynman rules involving the scalars which couple to top and bottom proportionally to the top-quark mass can be extracted from the Yukawa Lagrangian:

$$\begin{aligned}\mathcal{L}_Y &= -m_t\left[\bar{t}t + \frac{1}{\sqrt{2}v}(\bar{t}th_1 + \bar{b}bh_2) - \frac{i}{\sqrt{2}v}(\bar{t}\gamma_5 t\phi_1^0 + \bar{b}\gamma_5 b\phi_2^0)\right.\\ &+ \left.\frac{1}{v}\left(\bar{b}_L t_R \phi_2^- + \bar{b}_R t_L \phi_1^- + \bar{t}_L b_R \phi_1^+ + \bar{t}_R b_L \phi_2^+\right)\right] \qquad \text{(A4)}\end{aligned}$$

In terms of the physical scalars defined as in Eq. A3 the couplings we need become,

$$\begin{aligned}\mathcal{L}_Y &= -\frac{m_t}{v}\left[\cos\theta_R\left(\bar{b}P_R t H_1^- + \bar{t}P_L b H_1^+\right) + \frac{v_R}{\sqrt{v_R^2+v^2}}\left(\bar{b}P_L t H_2^- + \bar{t}P_R b H_2^+\right)\right.\\ &+ \left.\frac{1}{\sqrt{2}}\bar{b}\left(h_2 - iH_1^0\gamma_5\right)b\right]. \qquad \text{(A5)}\end{aligned}$$

The vertices of the form ZHH are obtained from the Lagrangian

$$\begin{aligned}\mathcal{L} &= \frac{ig_L}{2\cos\theta_W}\left(2\sin^2\theta_W - \frac{v_R^2}{v^2+v_R^2}\right)Z^\mu\left(H_2^-\partial_\mu H_2^+ - H_2^+\partial_\mu H_2^-\right)\\ &\quad \frac{-ig_L}{2\cos\theta_W}\cos 2\theta_W Z^\mu\left(H_1^-\partial_\mu H_1^+ - H_1^+\partial_\mu H_1^-\right)\\ &+ \frac{g_L}{2\cos\theta_W}Z^\mu\left(h_2\partial_\mu H_1^0 - H_1^0\partial_\mu h_2\right). \qquad \text{(A6)}\end{aligned}$$

Finally, the vertices of the form ZWH can be read from the Lagrangian

$$\mathcal{L} = -\frac{g_R^2}{\sqrt{2}}\frac{\sin\theta_R}{\sin\theta_W}\frac{vv_R}{\sqrt{v^2+v_R^2}}Z^\mu W_{R\mu}^{\pm}H_2^{\mp} \tag{A7}$$

4. Loops involving Gauge Bosons

Here we present results for the individual diagrams in Figure 1.

Diagram 1 a

To check our results we first evaluate this diagram for the case of the Standard Model in Unitary Gauge. In this case the internal wavy lines are W^+ and W^- and one finds,

$$\begin{aligned}\Gamma_\mu \;=\; & -i\frac{g}{2\cos\theta_W}\gamma_\mu\frac{g^2\cos^2\theta_W}{16\pi^2} \\ & \left(\frac{1}{\epsilon}\left(\frac{-M_Z^4}{12M_W^4}-\frac{4M_Z^2}{3M_W^2}+\frac{M_t^2M_Z^2}{4M_W^4}+\frac{3M_t^2}{2M_W^2}\right)+fa_L\right)P_L\end{aligned} \tag{A8}$$

Notice that the first two divergent terms in Eq. A8 that are not proportional to M_t^2 are not included in the finite quantity δg_{Lb} of Eq.28. These divergent terms cancel against other contributions from the renormalization of G_F, M_Z and α when one calculates observables such as the partial Z width [22]. It is possible to obtain a simple expression for the finite part fa_L in the limit $M_W^2/M_t^2 << 1$. It is given by,

$$fa_L \approx -\frac{M_t^2}{8M_W^2}\left(\frac{1}{\cos^2\theta_W}\left(2\log\left(\frac{M_t^2}{M_Z^2}\right)-3\right)+12\log\left(\frac{M_t^2}{M_Z^2}\right)-10\right) \tag{A9}$$

For our model, the terms that are enhanced by $\cot^2\theta_R$ are obtained when the internal wavy lines are W_R^+ and W_R^-, resulting in,

$$\begin{aligned}\Gamma_\mu \;=\; & -i\frac{g}{2\cos\theta_W}\gamma_\mu\frac{-g_R^2\sin^2\theta_W}{16\pi^2} \\ & \left(\frac{1}{\epsilon}\left(\frac{-M_Z^4}{12M_{W_R}^4}-\frac{4M_Z^2}{3M_{W_R}^2}+\frac{M_t^2M_Z^2}{4M_{W_R}^4}+\frac{3M_t^2}{2M_{W_R}^2}\right)+fa_R\right)P_R\end{aligned} \tag{A10}$$

The first two divergent terms in this expression, the ones not proportional to M_t^2, do not contribute to the vertex correction δg_{Rb} that we are computing because they are not enhanced by $\cot^2\theta_R$. Although they appear to be proportional to g_R^2, they really are not when one considers the relations from Eq. 18. The finite part can be calculated numerically (we only

present these results for the sum of all diagrams). For example, for $M_{W_R} = 500$ GeV, we find $fa_R = 1.32$ with a renormalization scale $\mu = M_Z$.

It is possible to present approximate analytical results by taking $M_Z = 0$ in the integrals. Doing so and expanding the resulting expression in powers of $M_t^2/M_{W_R}^2$ we find,

$$-i\frac{g_L}{2\cos\theta_W}\frac{g_R^2}{16\pi^2}(-\sin^2\theta_W)\left[\frac{3}{2}\frac{M_t^2}{M_{W_R}^2}\frac{1}{\epsilon}+\frac{3}{2}+\frac{M_t^2}{M_{W_R}^2}\left(\frac{11}{4}-\frac{3}{2}\log\left(\frac{M_{W_R}^2}{\mu^2}\right)\right)\right] \tag{A11}$$

Diagram 1 b

Once again we first evaluate Diagram b in Figure 1 for the Standard Model in unitary gauge. In that case the internal wavy line is a charged W and the intermediate state quarks are top. The result can be written in the limit $M_W^2/M_t^2 << 1$ as,

$$\begin{aligned}\Gamma_\mu &= -i\frac{g}{2\cos\theta_W}\gamma_\mu\frac{g^2|V_{tb}|^2}{16\pi^2}\frac{M_t^2}{M_W^2}\left(\left(-\frac{1}{\epsilon}\log\left(\frac{M_t^2}{M_Z^2}\right)-\frac{1}{2}\right)g_{Lt}\right.\\ &+\left.\left(\frac{1}{4\epsilon}-\frac{1}{4}\log\left(\frac{M_t^2}{M_Z^2}\right)-\frac{1}{8}\right)g_{Rt}\right)P_L\,.\end{aligned} \tag{A12}$$

For our model the only terms enhanced by $\cot^2\theta_R$ are obtained with the intermediate wavy line representing a $W_R^\pm$ and the intermediate state quark being top. As before, we present an approximate analytical result obtained by setting $M_Z = 0$ in the loop integrals and expanding the resulting expression in powers of $M_t^2/M_{W_R}^2$. This yields,

$$\begin{aligned}&-i\frac{g_L}{2\cos\theta_W}\frac{g_R^2}{16\pi^2}\left\{\frac{1}{\epsilon}\frac{M_t^2}{M_{W_R}^2}\left(\frac{g_{Lt}}{4}-g_{Rt}\right)-\frac{3}{4}g_{Rt}\right.\\ &\left.+\frac{M_t^2}{M_{W_R}^2}\left[\left(\log\left(\frac{M_t^2}{\mu^2}\right)-\frac{1}{2}\right)g_{Rt}-\frac{1}{4}\left(\log\left(\frac{M_t^2}{\mu^2}\right)+3\log\left(\frac{M_t^2}{M_{W_R}^2}\right)+\frac{7}{2}\right)g_{Lt}\right]\right\}\end{aligned} \tag{A13}$$

We only consider the case with $M_Z \neq 0$ numerically and include it in the sum of all diagrams in Figure 4.

Diagram 1 c

Finally we evaluate the wave-function renormalization diagrams of Figure 1 c. Once again we begin by considering the Standard Model in unitary gauge. For this diagram we can present an exact analytical result,

$$1 - Z_b^{-1} = \frac{g^2}{16\pi^2}P_L\left(\frac{3M_t^2}{4M_W^2}\frac{1}{\epsilon}-\frac{3M_t^2}{4M_W^2}\log\left(\frac{M_t^2}{\mu^2}\right)\right.$$

$$- \frac{3M_t^2 M_W^2}{4(M_t^2 - M_W^2)^2} \log\left(\frac{M_W^2}{M_t^2}\right) - \frac{6M_W^4 + 5M_t^2 M_W^2 - 5M_t^4}{8M_W^2(M_t^2 - M_W^2)}\Bigg) \qquad \text{(A14)}$$

Similarly, for the case of our model, the terms that are enhanced by $\cot^2\theta_R$ are obtained from the exchange of charged $W_R^\pm$ gauge bosons and we find,

$$\begin{aligned} 1 - Z_b^{-1} \;=\; & \frac{g_R^2}{16\pi^2} P_R \left(\frac{3M_t^2}{4M_W^2}\frac{1}{\epsilon} - \frac{3M_t^2}{4M_W^2}\log\left(\frac{M_t^2}{\mu^2}\right)\right. \\ & - \frac{3M_t^2 M_W^2}{4(M_t^2 - M_W^2)^2} \log\left(\frac{M_W^2}{M_t^2}\right) - \frac{6M_W^4 + 5M_t^2 M_W^2 - 5M_t^4}{8M_W^2(M_t^2 - M_W^2)}\Bigg) \qquad \text{(A15)} \end{aligned}$$

As a check of our calculation we have evaluated the corresponding expressions for the Standard Model in unitary gauge. From these we can obtain, by adding the three contributions, the vertex correction terms δg_{Lb} proportional to M_t^2. This result, Eq. 28, is finite and in agreement with the known result [18].

5. Loops with Scalar Mesons

We now turn our attention to the diagrams in Figure 2. As described in the main text we use the basis of Eq. A3 assuming all scalars to be degenerate and to have a large mass.

Diagram 2 a

This type of diagram involves one gauge boson and one physical charged scalar in the loop. There is only a contribution to the right-handed coupling involving the $W_R^\pm H_2^\mp$ intermediate state. Our result in the limit where the Higgs masses are much larger than other masses is:

$$-i\frac{g_L}{2\cos\theta_W}\frac{1}{16\pi^2}\left(\frac{m_t}{v}\right)^2\left(\frac{1}{\epsilon} + \frac{3}{2} - \log\left(\frac{M_H^2}{\mu^2}\right)\right) x_v(1-x_v)P_R \qquad \text{(A16)}$$

Diagram 2 b

This type of diagram involves two scalars in the intermediate state. The left-handed coupling receives contributions from charged H_1 scalars as well as from a diagram with one neutral H_1^0 pseudo-scalar and one h_2 neutral scalar. The right-handed coupling receives contributions from the same diagram with neutral scalars as well as from the diagram with

charged H_2 scalars.

$$-i\frac{g_L}{2\cos\theta_W}\frac{1}{16\pi^2}\left(\frac{m_t}{v}\right)^2\left(\frac{1}{\epsilon}+\frac{1}{2}-\log\left(\frac{M_H^2}{\mu^2}\right)\right)$$
$$\left[\left(\sin^2\theta_W+\cos^2\theta_W x_v-\frac{1}{2}x_v^2\right)P_R+\left(-\frac{1}{2}-\frac{\cos^2\theta_R}{2}\cos 2\theta_W\right)P_L\right] \qquad \text{(A17)}$$

Diagram 2 c

This type of diagram involves the exchange of a charged H_1 or of a neutral H_1^0 or H_2 scalars for the left-handed coupling as well as exchanges of a charged H_2 scalar or a neutral A_1^0 or H_2 scalars for the right-handed coupling.

$$-i\frac{g_L}{2\cos\theta_W}\frac{1}{16\pi^2}\left(\frac{m_t}{v}\right)^2\left(\frac{1}{\epsilon}+\frac{1}{2}-\log\left(\frac{M_H^2}{\mu^2}\right)\right)$$
$$\left[\left(-\frac{1}{3}\sin^2\theta_W+(-\frac{1}{2}+\frac{2}{3}\sin^2\theta_W)x_v\right)P_R+\left(\frac{1}{3}\sin^2\theta_W(1-2\cos^2\theta_R)\right)P_L\right] \qquad \text{(A18)}$$

Diagram 2 d

This diagram represents b wave-function renormalization through scalar loops. Once again, for the left-handed coupling one obtains contributions from exchanging a charged H_1 and neutral H_1^0 and H_2, whereas for the right-handed coupling the contributions arise through exchange of charged H_2 and neutral H_1^0 and H_2 scalars.

$$-i\frac{g_L}{2\cos\theta_W}\frac{1}{16\pi^2}\left(\frac{m_t}{v}\right)^2\left(\frac{1}{\epsilon}+\frac{1}{2}-\log\left(\frac{M_H^2}{\mu^2}\right)\right)$$
$$\left[\left(-\frac{2}{3}\sin^2\theta_W+\frac{1}{3}\sin^2\theta_W x_v\right)P_R+\left((1+\cos^2\theta_R)(\frac{1}{2}-\frac{1}{3}\sin^2\theta_W\right)P_L\right] \qquad \text{(A19)}$$

---

[1] D. Abbaneo *et al.* [ALEPH Collaboration], arXiv:hep-ex/0112021.

[2] K. Hagiwara *et al.* [Particle Data Group Collaboration], Phys. Rev. D **66**, 010001 (2002).

[3] M. S. Chanowitz, Phys. Rev. Lett. **87**, 231802 (2001) [arXiv:hep-ph/0104024].

[4] M. S. Chanowitz, Phys. Rev. D **66**, 073002 (2002) [arXiv:hep-ph/0207123].

[5] G. Altarelli, F. Caravaglios, G. F. Giudice, P. Gambino and G. Ridolfi, JHEP **0106**, 018 (2001) [arXiv:hep-ph/0106029].

[6] P. Bamert, C. P. Burgess, J. M. Cline, D. London and E. Nardi, Phys. Rev. D **54**, 4275 (1996) [arXiv:hep-ph/9602438].

[7] C. H. Chang, D. Chang and W. Y. Keung, Phys. Rev. D **54**, 7051 (1996) [arXiv:hep-ph/9601326].

[8] D. Chang and E. Ma, Phys. Rev. D **58**, 097301 (1998) [arXiv:hep-ph/9805273].

[9] D. Choudhury, T. M. Tait and C. E. Wagner, Phys. Rev. D **65**, 053002 (2002) [arXiv:hep-ph/0109097].

[10] G. Burdman and D. Kominis, Phys. Lett. B **403**, 101 (1997) [arXiv:hep-ph/9702265].

[11] C. X. Yue, Y. P. Kuang, X. L. Wang and W. B. Li, Phys. Rev. D **62**, 055005 (2000) [arXiv:hep-ph/0001133].

[12] G. Triantaphyllou, J. Phys. G **26**, 99 (2000) [arXiv:hep-ph/9811250].

[13] D. J. Muller and S. Nandi, arXiv:hep-ph/9610404.

[14] E. Malkawi and C. P. Yuan, Phys. Rev. D **61**, 015007 (2000) [arXiv:hep-ph/9906215].

[15] E. Malkawi, T. Tait and C. P. Yuan, Phys. Lett. B **385**, 304 (1996) [arXiv:hep-ph/9603349].

[16] K. R. Lynch, E. H. Simmons, M. Narain and S. Mrenna, Phys. Rev. D **63**, 035006 (2001) [arXiv:hep-ph/0007286].

[17] X. G. He and G. Valencia, Phys. Rev. D **66**, 013004 (2002) [Erratum-ibid. D **66**, 079901 (2002)].

[18] G. . Altarelli, R. . Kleiss and C. . Verzegnassi,

[19] R.N. Mohapatra and J.C. Pati, Phys. Rev. **D11**, 566(1975); Phys. Rev. **D11**, 2558(1975); R.N. Mohapatra and G. Senjanovic, Phys. Rev. **D12**, 1502(1975).

[20] K. S. Babu, X. G. He and E. Ma, Phys. Rev. D **36**, 878 (1987).

[21] A. Pukhov *et al.*, arXiv:hep-ph/9908288.

[22] S. Dawson and G. Valencia, Nucl. Phys. B **439**, 3 (1995) [arXiv:hep-ph/9410364].

[23] Notice that there is a factor of 2 difference between the definitions of δg_R here and in Ref. [17].

[24] recall that the dependence of this amplitude on $\cot\theta_R$ is only through the width of the Z'